یازدهمین کنگره ملی سراسری
فناوریهای نوین در حوزه توسعه پایدار ایران
11th National Congress of
the New Technologies in Sustainable Development of Iran
senaconf.ir

# Detect the Intensity of Disturbance Based on Inertia Estimation

Saman Mahmoodi
University of Kurdistan
Sanandaj, Kurdistan
saman.mahmoodi@uok.ac.ir

*Abstract*—**There are always different disturbances in the power grids. The efficacy of system generators to disturbance depends on the severity and location. Obviously, if the severity of disturbance is higher, system generators are more affected. Moreover, considering the location of its occurrence, the influence of the generators will be different. On the other hand, the presence of renewable energy sources(RES) such as solar photovoltaic(SPV), wind turbines (WT) has increased. As a result, power network becomes vulnerable and more prone to protection issues. Therefore, if the intensity of disturbance(IOD) is detected, it can be prevented from the damage to equipment of network and generators. In this paper, a solution to measure the intensity of disturbances in the power system has been proposed. The proposed method consists of two important factors, including inertia system and frequency variations. The inertia of each generator acts as a hard factor against disturbance. According to renewable energy sources that have low inertia or lack of inertia, it is necessary to know the inertia of each generator to detect the severity of the disturbance. So, the presented method is based on inertial estimation. In this method at first, the moment of the disturbance is detected, and based on the modified swing equation, the system inertia is estimated. Then, using estimated inertia and system frequency measurements, the disturbance intensity is determined for each generator. To study the presented method, a proposed single-machine and IEEE 39-bus test system has been used.**

***Keywords- inertia estimation, the intensity of disturbance, inverter-based generators, renewable energy sources, the start of disturbance.***

## 1. Introduction

Today, renewable energy sources like solar photovoltaic and wind turbines in power systems are increasing. Usually, these sources are connected to the power grids with power electronics interfaces. So, no response from inertia. System inertia is the inherent characteristic of each generator and the first factor against changes in system frequency [1]. Considering these issues, the connection of these resources to the power system will create challenges. Moreover, knowing the system inertia can be a great help in dealing with probabilistic problems for stability protection issues. At first, some of the tasks that have attempted to investigate the problem of inertia estimation, are presented. In the beginning, the system inertia was estimated offline. In this work, the spinning reservation problem was examined [2]. Due to the presence of renewable sources, system inertia faces new challenges. Therefore, the estimation of inertia in wind turbines based on induction generators is investigated [3]. In the next years, an online estimate has been developed and the system inertia is estimated to be static and dynamic. The static estimation is based on the swing equation and in dynamic estimation, system parameters identification is necessary [4]. The first statistical model was to estimate the inertia of the Gaussian model [5]. In [6,7], the proposed method for inertial estimation is based on system identification. This method offers a robust estimation. With the development of measurement devices, such as wide-area measurements(WAMs) and phasor measurement units(PMUs), system inertia was carried out with high precision and online [8,9]. Various factors affect the accuracy of the estimation. One of the most important of these factors is recognition of the moment of disturbance occurrence [10,11]. Nevertheless, more sensitivity was found on a method for accurate detection of the moment of disturbance. Due to this, a method based on the creation of a structural frame for the effectiveness of the generators connected to the power network from disturbance events was presented [12]. Using of wide-area measurements makes the propagation of disturbance in power systems more obvious. Accordingly, if the spread of disturbance propagation is measured, it's possible to prevent damage to the main part of the system [13]. As mentioned, the response of the generators connected to the system is different from the severity of disturbance. Whatever IOD was higher, the generators become more excited. In contrast, the generators are also less excited. Nevertheless, the accuracy of the estimation in the occurrence of small disturbances must be more accurate in the occurrence of a large disturbance. So, a closed-loop identification method based on sinusoidal signals is proposed to estimate the system inertia under small disturbance [14]. Recently, With the advancement of measurement technology and its availability in laboratories, it has paved the way for engineers to test the proposed methods [15]. In this reference, a robust method for estimation of inertia according to the presence of renewable sources like the solar system and wind turbine has been offered. Other parts of this paper are organized as follows. Other parts of this paper are organized as follows.

In the next section, the proposed method is expressed to estimate the inertia. In section 3, the results are discussed by applying the proposed method to the test system. Finally, section 4 is allocated to the results.

## 2. The Proposed Method for The Estimation of Inertia

In this paper, an online method for detecting IOD based on estimation of inertia is proposed. In this method, in addition to the estimation of inertia, the damping coefficient and mechanical power of each generator are estimated. Due to the presence of inverter-based generators, system inertia has changed so much. Thus, an estimate of inertia can help identify the system inertia. Inertia is measured in the first moments when the system responds to the occurrence of disturbance. Therefore, there must be sufficient knowledge of the occurrence of disturbance. In this regard, a method for detecting the start of disturbance (SOD) is proposed, and is formulated as follows [16]:

$$\begin{aligned} S_i(t) &= \left(f_i(t) - \overline{f(t)}\right)^2 \\ SOD_i(t) &= S_i(t+t_0) - S_i(t) > 0 \end{aligned} \quad (1)$$

Where, $f_i(t)$ is the frequency measured in bus $i$, and $\overline{f(t)}$ is average frequency measured up to the moment the data is received. Therefore, when the $SOD_i$ is greater than zero, time is the start of disturbance. To ensure that there is an Event of disturbance, the amount of $SOD_i(t)$ is calculated for several instances of the disturbance occurrence. Usually, the next five samples are calculated. However, help($SOD_i\_h$) equation is introduced as the following:

$$\begin{aligned} SOD_i\_\hat{h}(t) &= \exp(\delta_i(t) - \overline{\delta_i}(t_n)) \\ SOD_i\_h(\mathrm{t}) &= \left|SOD_i\_\hat{h}(t+t_0) - SOD_i\_\hat{h}(t)\right| \geq 1 \end{aligned} \quad (2)$$

In this equation, $\delta_i(t)$ is the angle measured in bus $i$ at the moment $t$ and $\overline{\delta_i}(t_n)$ the mean angle of bus $i$ to the moment $t_n$. $n$ is the number of sample measurements. After finding the start of disturbances, system inertia is estimated. Accordingly, the swing equation is first rewritten as [17]:

$$2H_i \frac{d\omega_i}{dt} = P_{m_i} - P_{e_i} - D_i(\omega_i - \omega_0) \quad (3)$$

Where, $P_{m_i}$ and $P_{e_i}$ is the mechanical power supplied by the generator and the electric power demand respectively. $H_i$ is the inertia constant of the generator $i$ in seconds and D is the damping factor. The rotor speed variation is denoted $\frac{d\omega_i}{dt}$. It is assumed:

$$\frac{d\omega_i}{dt} = \wp\omega_i \quad \Rightarrow \quad \frac{d\omega_i}{dt} = \wp 2\pi f_i \quad \Rightarrow \quad \wp = \frac{d\omega_i}{dt}\Big/ 2\pi f_i \quad (4)$$

In Eq. 4, $\wp$ ratio of rotor speed changes to frequency measured in bus $i$. So, the swing equation is modified as follow:

$$\begin{aligned} 2H_i \wp 2\pi f_i &= P_{m_i} - P_{e_i} - D_i(2\pi f_i - 2\pi f_0) \\ 4\pi H_i \wp f_i + 2\pi D_i f_i &= P_{m_i} - P_{e_i} + 2\pi D_i f_0 \end{aligned} \quad (5)$$

Thus:

$$f_i = \frac{P_{m_i}}{(4\pi H_i \wp + 2\pi D_i)} - \frac{P_{e_i}}{(4\pi H_i \wp + 2\pi D_i)} + \frac{2\pi D_i f_0}{(4\pi H_i \wp + 2\pi D_i)} \quad (6)$$

With simplifying the above equation:

$$f_i = \Upsilon_{1_{1_i}} + P_{e_i}\Upsilon_{2_i} + 2\pi f_0\, \Upsilon_{3_i} \quad (7)$$

Where, $\Upsilon_1$ , $\Upsilon_2$ and $\Upsilon_3$ parameters are:

$$\Upsilon_{1_i} = \frac{P_{m_i}}{(4\pi H_i \wp + 2\pi D_i)} \quad and \quad \Upsilon_{2_i} = \frac{1}{(4\pi H_i \wp + 2\pi D_i)} \quad and \quad \Upsilon_{3_i} = \frac{D_i}{(4\pi H_i \wp + 2\pi D_i)} \quad (8)$$

As result, $P_m$ , D and H will be obtained as follows:

$$P_{m_i} = \frac{\Upsilon_{1_i}}{\Upsilon_{2_i}} \quad and \quad D_i = \frac{\Upsilon_{3_i}}{\Upsilon_{2_i}} \quad and \quad H_i = \frac{1}{2\pi \wp \Upsilon_{2_i}}\left(1 - 2\pi \Upsilon_{3_i}\right) \quad (9)$$

Finally, the swing equation is modified in a linear-regression equation that is a function of the frequency:

$$f_i(t) = \begin{bmatrix} 1 & P_{e_i} & 2\pi f_0 \end{bmatrix} \begin{bmatrix} \Upsilon_{1_i} \\ \Upsilon_{2_i} \\ \Upsilon_{3_i} \end{bmatrix} + E_i \quad (10)$$

Where, $E_i$ is measurement error. Given the minimization of Eq. 10, the unknown values are estimated [16,18]. Accuracy of estimating the unknown parameters is dependent on fitting carefully of the system frequency variations. As the accuracy of the curve fitting was higher, also the accuracy of estimating unknown parameters is high. Error estimation of inertia obtained as follow:

$$E_{est\,i}\,(\%) = \frac{\left|H_{i_{esttimation}} - H_{i_{actual}}\right|}{\left|H_{i_{actual}}\right|} \times 100 \quad (11)$$

Where, $H_{i_{estimation}}$ is inertia estimation in generator connected to bus $i$, and $H_{i_{actual}}$ is the actual inertia in the generator connected to bus $i$. The flowchart of the proposed method for IOD is based on the estimation of inertia shown in Figure 1.

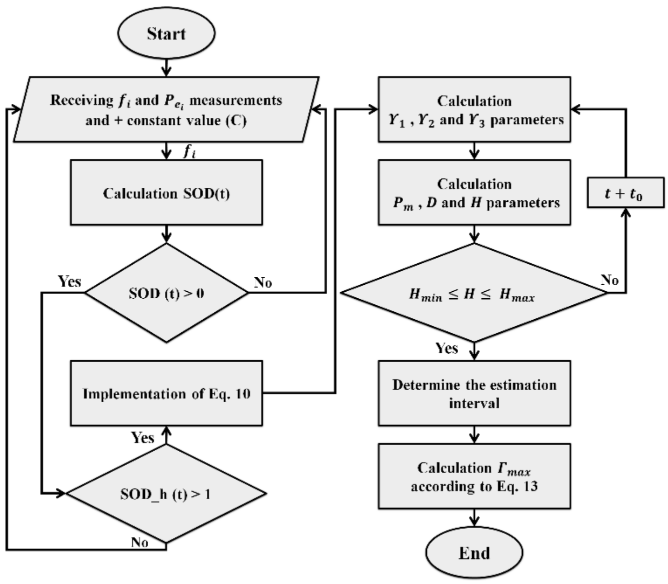


Figure 1. The flowchart of the proposed method for IOD based on estimation of inertia

After estimation of inertia, IOD applied to each generator is determined. For this purpose, the following equations are used:

$$[\Gamma]_{kl} = \begin{bmatrix} \Gamma_{11} & \cdots & \Gamma_{1l} \\ \vdots & \ddots & \vdots \\ \Gamma_{k1} & \cdots & \Gamma_{kl} \end{bmatrix}_{k\times l} \quad and \quad \Gamma_{kl} = \left(f_{kl} - \overline{f_{k-l}}\right)^2 \qquad (12)$$

$$[\Gamma]_{N_{max}} = \begin{bmatrix} max(\Gamma_1) \times \sqrt{\dfrac{2\pi\wp\Upsilon_{2_i}}{(1-2\pi\Upsilon_{3_i})}} \\ \vdots \\ max(\Gamma_k) \times \sqrt{\dfrac{2\pi\wp\Upsilon_{2_N}}{(1-2\pi\Upsilon_{3_N})}} \end{bmatrix}_{N\times 1} \qquad (13)$$

Where, $f_{kl}$ is the frequency of bus $k$, and $l$ is sample measured in bus $k$, and $\overline{f_{k-l}}$ is average frequency measured in bus $k$ and up to the $l$ sample received. $H_N$ is the generator inertia constant connected to bus $N$. Therefore, IOD is determined according to Eq. 12.

## 3. Case Studies and Numerical Simulation

In this paper, the proposed single–machine system and IEEE 39-bus test system are used to investigate the proposed method of inertia estimation. The single–machine system contains one synchronous generator, two buses, and a PQ load that is connected through a line to the generator. The detail of the system is listed in appendix A. IEEE 39-bus test system consists of 10 synchronous generators, and each generator is equipped with the excitation type 2 system. The conventional system parameters are selected from in [19]. In continue, these systems are more explained.

### *3.1. The single–machine system proposed*

The main reason for using such a system is more simple to understand the effect of inverter-based generators on system inertia and disturbance intensity. In this paper, Photovoltaic Solar System is modeled as an inverter-based generator. Like Figure 2, the inverter-based generators are integrated with the study system [20].

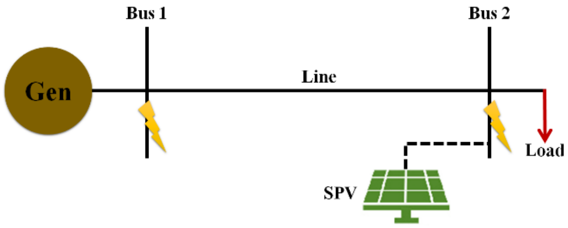


Figure 2. The single-machine system proposed

For this purpose, four cases where their occurrence locations are nearly and far away from a generator in the system with and without an inverter-based generator are considered.

**Case 1:** a three-phase fault has occurred at t=1.1s and it is cleared at t=1.3s on bus number 1 in the system without the inverter-based generator.

**Case 2:** a three-phase fault has occurred at t=1.1s and it is cleared at t=1.3s on bus number 2 in the system without the inverter-based generator.

**Case 3:** a three-phase fault has occurred at t=1.1s and it is cleared at t=1.3s on bus number 1 in the system with an inverter-based generator.

**Case 4:** a three-phase fault has occurred at t=1.1s and it is cleared at t=1.3s on bus number 2 in the system with an inverter-based generator.

In Figure 3, the moment of the occurrence of disturbance is shown. As seen, the detection of this moment in both methods is the same, and the disturbance occurs at the moment of 1.1 second.

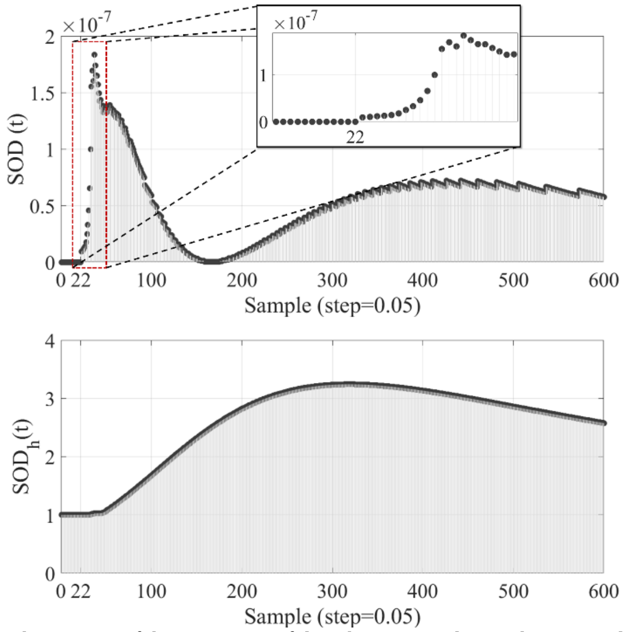


Figure 3. The moment of the occurrence of disturbance according to the proposed methods

Different cases were investigated on the case study system. The results regarding the estimation of inertia, damping factor, and mechanical power are listed in Table 1. The system inertia reduction in the presence of inverter-based generators is obvious. As also shown in Figure 4.

Table 1. Estimation of Inertia, damping factor, and mechanical power

| Case/Est | $H_{est}$ | $D_{est}$ | $Pm_{est}(p \cdot u)$ | Error of Inertia Estimation(%) |
|---|---|---|---|---|
| Case 1 | 5.49 | 2.67 | 0.84 | 0.9 |
| Case 2 | 5.47 | 2.43 | 0.81 | 0.7 |
| Case 3 | 4.98 | - | 0.63 | - |
| Case 4 | 5.02 | - | 0.64 | - |

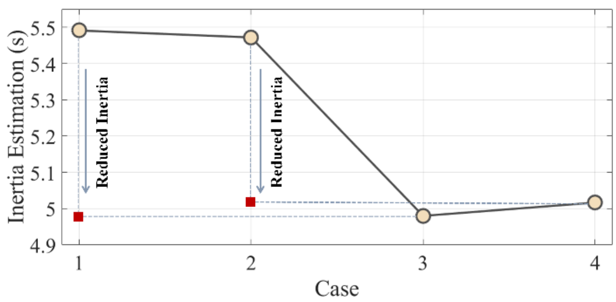


Figure 4. Inertia estimation for different cases

However, it should be noted whether the system inertia reduction affects IOD applied to the generator? To answer this question, Figure 5 is plotted. According to Eq.13, IOD depended on two factors. These factors are inertia and frequency variations. IOD increases with the rise in frequency variations and the reduction of inertia. So, it is expected that by decreasing the inertia, IOD applied to the generator increases. But, this intensity is reduced.

When an inverter-based generator is connected to the system, the power generated by the conventional generator decreases. As shown in Figure 6. Thus, frequency variations are reduced through the swing equation. On the other hand, the inertia of the system has decreased. However, since the frequency variations have more effect on disturbance intensity, the intensity applied to the generator is reduced. Finally, in terms of system protection issues, using renewable sources, such as inverter-based generators, can reduce the severity of disturbance imported to any generator and prevent damage to system components, and in terms of system stability, stability can be improved.

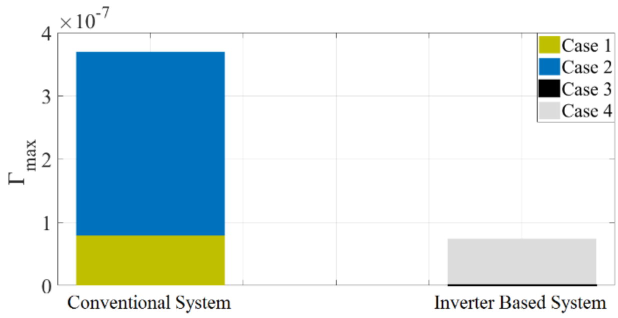

Figure 5. IOD applied to the generator in a conventional and inverter-based system

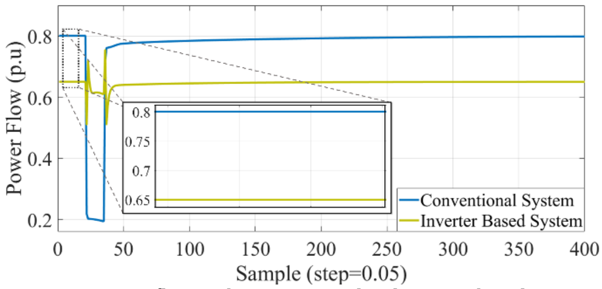

Figure 6. Power flow in the conventional and inverter-based system

*3.2. IEEE 39-bus test system*

In this study, the IEEE 39-bus test system has been used to verify the proposed method and its application in larger systems (as shown in Figure 7). To study the proposed method, four cases are considered at different points of the system.

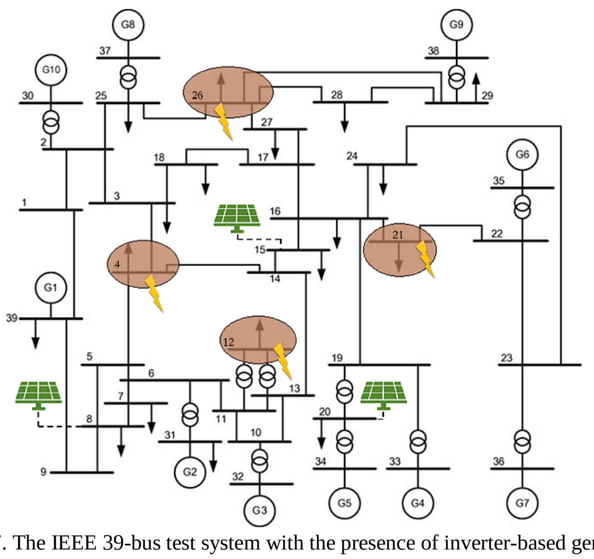
Figure 7. The IEEE 39-bus test system with the presence of inverter-based generators

**Case 1:** a three-phase fault has occurred at t=1.1s and it is cleared at t=1.2s on bus number 21 in the system with and without an inverter-based generator.
**Case 2:** a three-phase fault has occurred at t=1.1s and it is cleared at t=1.2s on bus number 26 in the system with and without an inverter-based generator.
**Case 3:** a three-phase fault has occurred at t=1.1s and it is cleared at t=1.2s on bus number 4 in the system with and without an inverter-based generator
**Case 4:** a three-phase fault has occurred at t=1.1s and it is cleared at t=1.2s on bus number 12 in the system with and without an inverter-based generator.

The results of inertia and error estimation in the conventional system are shown in Figure 8 and Figure 9, respectively. The outcome of inertia estimation for cases is nearly and this verifies the accuracy of the proposed method. The error estimation for all cases is illustrated in the box diagram. The mean error estimation for all generators is smaller than 7% and for the majority of generators, it is less than 5 %.

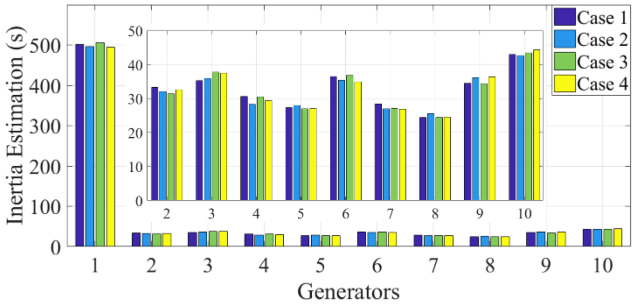


Figure 8. Inertia estimation of generators for all cases in a conventional system

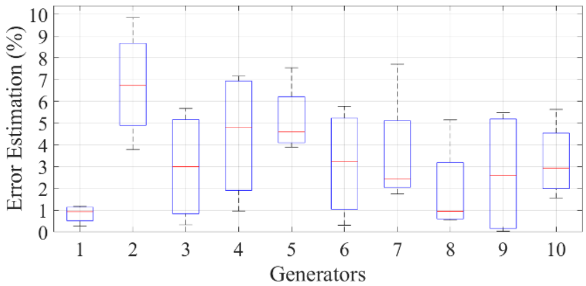


Figure 9. Error estimation of inertia of the generators for all cases in a conventional system

After accurate estimation of inertia, the problem of IOD is investigated. This issue is shown in Figure10. In the first case, the fault occurs on bus 21, and the generator connected to bus 35(generator 6) is expected to be more affected due to proximity to the fault event location, but, the generator connected to bus 34(generator 5) takes more IOD. Therefore, it can be concluded that the generator near the location of the disturbance will not be the most affected. For the second case, the generator connected to bus 38(generator 9) is the most IOD and followed by the generator connected to bus 37(generator 8), and other generators are classified as shown. The third and fourth cases have similar results and the connected generators of a system have a similar effect of IOD. The significant note is that the location of the error occurring in both cases is close to the generator connected to bus 39(generator 1), however, this generator has the least effect on fault. Due to the high inertia of this generator, the effect of this inertia is considered in Eq. 13. In all cases, the inertia effect of each generator on the severity of the disturbance is quite evident.

By studying the conventional system, the effect of inverter-based generators on the results of system inertia and disturbance intensities has been considered. Like Figure 7, the inverter-based generators are integrated with the study system. The SPV-1 capacity is 100 MW, The SPV-2 capacity is 150 MW and The SPV-3 capacity is 200 MW. According to the box plot in Figure 11, inertia estimation of the system for all cases with the presence of inverter-based generators is recused.

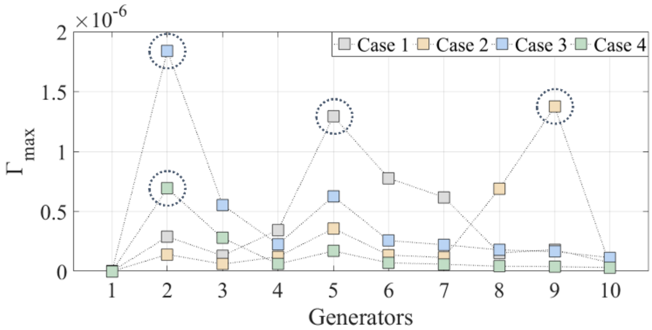

Figure 10. IOD applied to the generator in a conventional system

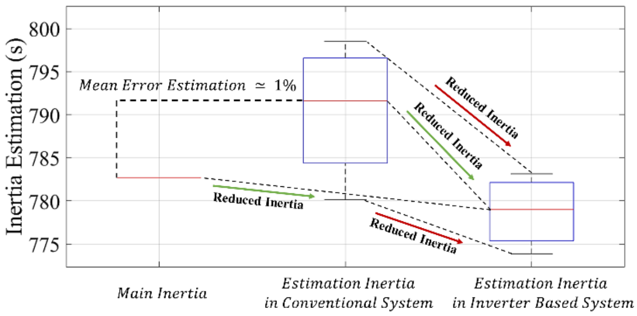

Figure 11. System inertia estimation concerning the presence of inverter-based generators for all cases

According to inertia reduction, certainly, IOD applied to the generators are changed. As shown in Figure 12 and Figure 13, two major changes have occurred. First, the rate of disturbance intensity has decreased to any generators. Second, the classification of generator 2 has changed in all cases.

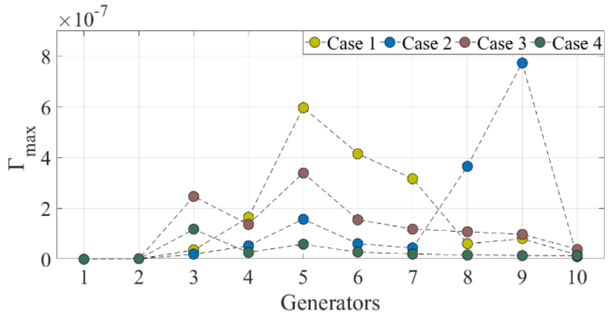

Figure 12. IOD applied to the generator in an inverter-based system

As described in the single-machine system, IOD depended on two factors. The reduction of inertia is obvious. On the other hand, the frequency variation in the inverter-based system has decreased (As seen in Figure 14 and Figure 15). Therefore, this is a compelling reason to reduce IOD applied to the system generators. As shown in the Figures, frequency variations of generator 2 have been greatly reduced. This reason for a change of classification of generator 2 in all cases. Moreover, in the conventional system for case 1, frequency variations of generator 2 are higher. But in an inverter-based system, it's not like and generator 5 is higher. This result was illustrated in Figure 13.

| Case 1 CS | Case 1 IBS | Case 2 CS | Case 2 IBS | Case 3 CS | Case 3 IBS | Case 4 CS | Case 4 IBS |
|---|---|---|---|---|---|---|---|
| G5 | G5 | G9 | G9 | G2 | G5 | G2 | G3 |
| G6 | G6 | G8 | G8 | G5 | G3 | G3 | G5 |
| G7 | G7 | G5 | G5 | G3 | G6 | G5 | G6 |
| G4 | G4 | G2 | G6 | G6 | G4 | G6 | G4 |
| G2 | G9 | G6 | G4 | G4 | G7 | G4 | G7 |
| G9 | G8 | G4 | G7 | G7 | G8 | G7 | G8 |
| G8 | G3 | G7 | G3 | G8 | G9 | G8 | G9 |
| G3 | G10 | G3 | G10 | G9 | G10 | G9 | G10 |
| G10 | G2 | G10 | G2 | G10 | G2 | G10 | G2 |
| G1 | G1 | G1 | G1 | G1 | G1 | G1 | G1 |

Figure 13. Classification IOD applied to the generator in conventional(CS) and inverter-based system(IBS)

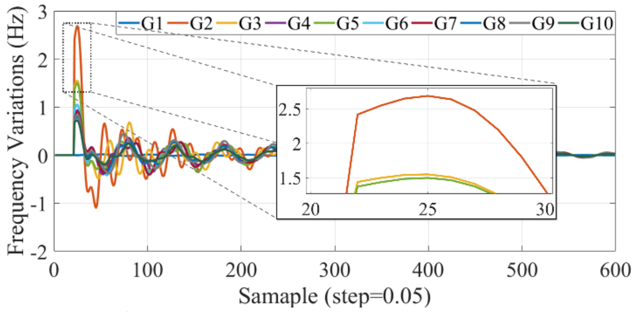


Figure. 14. Frequency variations of generators connected to the system without inverter-based generators for case 1

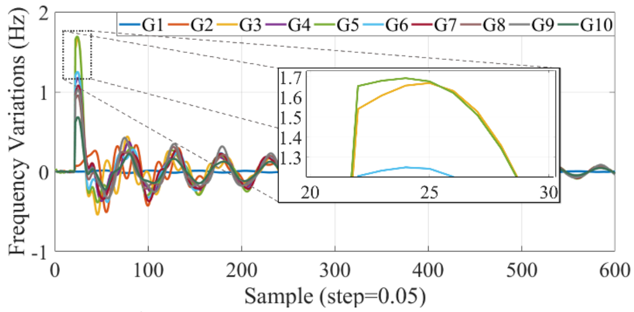


Figure. 15. Frequency variations of generators connected to the system with inverter-based generators for case 1

## 4. Conclusion

Always, power systems face different disturbances. If IOD is higher, the more likely it will be that the system equipment will be more vulnerable. Thus, it can contribute significantly to power system operators in adopting protection cases for the power system. This problem led to the presentation of a method based on the estimation of inertia for measuring IOD in this paper. To investigate the proposed method, a single-machine and IEEE 39-bus test system with the presence of renewable energy sources was used. Simulation results show that the presence of these sources reduces system inertia. But, it was observed that the intensity of disturbance is reduced in the inverter-based system. Due to the reduction of inertia, IOD is expected to decrease in two systems. The reason for this result is represented in the single-machine system. It is observed that with the presence of a solar photovoltaic system, power production by the conventional generator is reduced. This causes the system frequency Variations to decrease, thus the disturbance intensity is decreased. In IEEE 39 bus test system, the effect of fault event location on the disturbance intensity that applied to each generator was investigated. As observed that in the presence of renewable sources, classification of conventional generators based on IOS applied are change. usually, generators close to the location of the disturbances are more affected but this is not always the correct thing. The obtained observations confirm the accuracy of the proposed methods, and with the hope of using them in the proposed system and future works, we can consider issues such as virtual inertia and the effect of different loads' nature on proposed methods.

## References

[1] Erik Qrum, Mikko Kuivaniemi, Minna Laasonen, "Future system inertia", European Network of Transmission System Operators for Electricity (ENTSO-E) Report.
[2] Toshio Inoue, Haruhito Taniguchi, Iwado-Kita Komae-shi, Yasuyuki Ikeguchi, Kiyoshi Yoshida, Nakanoshima Kita-Ku, "Estimation of power system inertia constant and capacity of spinning-reserve support generators using measured frequency transients", IEEE Transactions on Power Systems, February 1997.
[3] T. Littler, B. Fox, and D. Flynn, "Measurement-based estimation of wind farm inertia", in Power Tech, IEEE Russia, 2005.
[4] P. Wall, F. González-Longatt, and V. Terzija, "Estimation of generator inertia available during a disturbance", presented at the IEEE Power Energy Soc. Gen. Meeting, San Diego, CA, USA, 2012.
[5] Xue Cao, Bruce Stephen, Ibrahim Abdulhadi, Campbell Booth, and Graeme M. Burt, "Switching Markov Gaussian Models for Dynamic Power System Inertia Estimation", 2016 IEEE. Translations and content mining are permitted for academic research only.
[6] Kaur Tuttelberg, Jako Kilter, Douglas Wilson, and Kjetil Uhlen, "Estimation of Power System Inertia from Ambient Wide Area Measurements", IEEE Transactions on Power Systems 2018.
[7] Junbo Zhao, Yi Tan, Vladimir Terzija, "Robust Online Estimation of Power System Center of Inertia Frequency", IEEE Transactions on Power Systems 2019.
[8] Peter Wall and Vladimir Terzija, "Simultaneous Estimation of the Time of Disturbance and Inertia in Power Systems", IEEE Transactions on Power Systems Delivery, Digital Object Identifier10.1109/TPWRD.2014.
[9] Yajun Wang, Horacio Silva-Saravia, Hector Pulgar-Painemal, "Estimating inertia distribution to enhance power system dynamics", This material is based on work supported by the National Science Foundation, 2017.
[10] Phillip M. Ashton, Christopher S. Saunders, Gareth A. Taylor, Alex M. Carter, and Martin E. Bradley, "Inertia Estimation of the GB Power System Using Synchrophasor Measurements", IEEE Transactions on Power Systems, 2015.
[11] J. D. Lara-Jimenez and Juan M. Ramirez, "Inertial Frequency Response Estimation in a Power System with High Wind Energy Penetration", 2015 IEEE Eindhoven PowerTech.
[12] Bi T, Qin J, Yan Y, et al, "An approach for estimating disturbance arrival time based on structural frame model", IEEE Trans Power Syst, 2017, 32: 1741–1750.
[13] J. S. Thorp, C. Seyler, and A. G. Phadke, "Electromechanical wave propagation in large electric power systems", IEEE Trans. Circuits Syst. I, Fundam. Theory Appl., vol.45, pp. 614-622, Jun. 1998.
[14] Guowei Cai, Bo Wang, Deyou Yang, Zhenglong Sun, Lixin Wang, "Inertia Estimation Based on Observed Electromechanical Oscillation Response for Power Systems", IEEE Transactions on Power Systems 2019.
[15] Rakesh Kumar Panda, Abheejeet Mohapatra, S. C. Srivastava, "Online Estimation of System Inertia in a Power Network utilizing Synchrophasor Measurements", IEEE Transactions on Power Systems, 2020.
[16] Saman Mahmoodi, Ali Hesami Naghshbandy, Rahmatollah Mirzaei, "An online method for inertia estimating and its application in coherency identification", 28th Iranian Conference on Electrical Engineering(ICEE) 2020.
[17] P. Kundur, Power System Stability, and Control. New York, NY, USA: McGraw-Hill, 1994.
[18] Jeffrey C. Lagarias, James A. Reeds, Margaret H. Wright, Paul E Wright, "Convergence Properties of the Nelder--Mead Simplex Method in Low Dimensions", Society for Industrial and Applied Mathematics, 1998.
[19] M. A. Pai, "Energy Function Analysis for Power System Stability", Power Electronics and Power Systems, Springer Science & Business Media, 2012.
[20] Prof. Federico Milano, "Power Systems Modelling and Control (EEEN40550)", Room 157a – Engineering & Materials Science Centre, 2019.

## Appendix A. The detail of the Single-machine system

Table 2. Single-machine proposed parameter

| | | | | |
|---|---|---|---|---|
| Generator | $X_d$ (p.u) | $\dot{X}_d$ (p.u) | $\dot{T}_{d0}$ (s) | $P_m$ (p.u) |
| | 2 | 0.3 | 8.0 | 0.8 |
| | $X_q$ (p.u) | $\dot{X}_q$ (p.u) | $\dot{T}_{q0}$ (s) | $P_{base}$ (MW) |
| | 1.8 | 0.5 | 0.8 | 100 |
| | $X_l$ (p.u) | $r$ (p.u) | H (s) | D (p.u) |
| | 0.05 | 0.001 | 5.5 | 2.5 |
| SPV | $T_p$ | $T_p$ | $K_v$ | $K_i$ |
| | 0.01 | 0.01 | 10 | 0.01 |
| Line | R (p.u) | $X_l$ (p.u) | $X_c$ (p.u) | F (Hz) |
| | 0.001 | 0.1 | 0.01 | 60 |
| Load | P (p.u) | Q (p.u) | $V_{min}$(p.u) | $V_{max}$(p.u) |
| | 0.8 | 0.4 | 0.9 | 1.1 |